Surfactant-Directed Synthesis of Mesoporous Titania with Nanocrystalline Anatase Walls and Remarkable Thermal Stability

Kristof Cassiers,*,† Thierry Linssen,† Mariska Mathieu,† Yuan Q. Bai,‡ Huai Y. Zhu,‡ Pegie Cool,†,§ and Etienne F. Vansant†

Department of Chemistry, Laboratory of Adsorption and Catalysis, University of Antwerp (UA), Universiteitsplein 1, B-2610 Wilrijk and Electron Microscope Unit & School of Chemistry, Madsen Building F09, The University of Sydney, NSW 2006, Australia

Received: September 22, 2003; In Final Form: January 19, 2004

A synthesis route to mesoporous titania with remarkable thermal stability was developed using an amine or cetyltrimethylammonium-templating procedure. By a treatment of the titania hybrids in aqueous ammonia, a method has been developed to overcome the lack of thermal stability above 350 °C. As for most mesoporous titanias described in the literature, this thermal instability originates from the uncontrolled phase transformation of amorphous template-free titania into massive anatase grains. In situ Raman spectroscopy, X-ray Diffraction, Differential Scanning Calorimetry and Thermogravimetrical Analysis demonstrated that parts of the amorphous titania walls of the NH_3-treated titania hybrids were transferred into walls built up of rutile nanobuilding blocks before the template was thermally removed. We further found that, after a subsequent increase of temperature to remove the template, the remaining amorphous particles were transformed into anatase in such a way that this crystallographic transformation is accompanied by a retention of the pore structure without massive segregation of anatase nuclei. This leads to ordered high surface area (up to 600 $m^2\ g^{-1}$) mesostructured titania having pore volumes up to 0.28 $cm^3\ g^{-1}$. XRD and N_2 adsorption−desorption data showed an outstanding thermal stability; the mesoscale order of NH_3-treated titanias was retained after thermal treatment up to 600 °C.

Introduction

The first successful combination of sol−gel chemistry and self-assembly by Mobil researchers generated a very impressive effort devoted to fundamental and practical research on ordered mesoporous silica.[1,2] Many studies have been reported concerning the preparation conditions, synthesis mechanism, characterization, and potential applications of these ordered templated mesoporous silicas.[3] However, extension of the surfactant templating process to the formation of nonsilica mesoporous oxides has been much less studied, although these compounds display very interesting and promising functionality for electrochemical applications and high surface area catalysis.

As one of the most important oxides, titania has been widely used in which many of the possible applications arise from the semiconductive nature of titania and the photoactivity of its anatase crystal phase.[4−6] Titania can be used as an electrode such as a dye-sensitized solar cell[7,8] or as a catalyst in organic reactions such as the oxidation of toluene or 1-butene, and so forth.[9−12] Furthermore, titania can be used in interesting applications in the treatment of polluents, such as the photocatalytic degradation of organic chloride compounds, and so forth.[13]

For the above applications, titania with large surface area and high porosity is favorable. Different synthetic strategies have been developed using a variety of templates, such as alkyl phosphate anionic surfactants,[14,15] quaternary ammonium cationic templates,[16−19] primary amines,[20−23] and poly(ethylene oxide)-based surfactants.[24−29] One of the major problems in the synthesis of TiO_2 based mesostructures is to achieve an adequate balance between the hydrolysis−condensation processes of the titanium precursor on one hand and the self-assembling reactions occurring between the resulting hydrolyzed supramolecular entities and the template on the other hand. The high reactivity of the available titanium sources toward hydrolysis and condensation leads to densely and poorly structured inorganic networks. To control the reactivity of titanium alkoxides, the addition of stabilizing agents such as bidentate ligands were used in the alkyl phosphate templated synthesis of mesostructured TiO_2.[20,30] Unfortunately, by using alkyl phosphate templates, a significant amount of phosphate remains in the calcined materials, which poisons the surface catalytic sites. Recently, phosphorus-free mesoporous titania was prepared in basic medium using quaternary ammonium surfactants in combination with triethanolamine as stabilizing agent,[18] resulting in a wormlike titania whereas hydrogen peroxide as hydrolysis−condensation inhibitor gives rise to lamellar or hexagonal TiO_2.[16] In slightly acidic conditions, mesoporous oxophosphates with hexagonal texture can be synthesized with quaternary ammonium surfactants[17] while pure phosphate-free titania was also prepared in neutral conditions with primary amines.[21−23] Recently, Stucky et al.[24] introduced a very efficient alternative synthetic approach to mesoporous transition metal oxides by using the so-called evaporation-induced self-assembly process (EISA). By slow alcohol evaporation, a controlled building of an inorganic network with nanocrystalline domains around the voids of the liquid-crystalline phase results in a well-defined hexagonally ordered TiO_2 mesophase. This method is also

* To whom correspondence should be addressed. E-mail: kristof.cassiers@ua.ac.be; fax: +32-3-820.23.74; tel: +32-3-820.23.75.
† University of Antwerp.
‡ The University of Sydney.
§ E-mail: pegie.cool@ua.ac.be.

10.1021/jp036830r CCC: $27.50
Published on Web 03/02/2004

successfully applied to other poly(ethylene)-based surfactants[26] and quaternary ammonium bromide as structure-directing agents.[19]

Next to a balance between the different reaction processes during synthesis, a controlled thermal treatment upon removal of the template as well as nucleation and growth of anatase domains is crucial since high porosity and a crystalline character of the TiO_2 particles are favorable for most applications. However, most reported syntheses of pure titania cited above have a very low thermal stability. Upon calcination at 300 or 350 °C, which is the bottom temperature to remove the template, BET surface areas reach very high values up to 600 $m^2\ g^{-1}$. Heat treatment at temperatures higher than 350 °C induces a remarkable collapse of the pore system because of phase transformation from amorphous titania to anatase. Only in titania directed with poly(ethylene oxide)-based templates could higher temperatures be reached without collapse of the mesophase.[24−29] Gedanken et al.[21] obtained a surface area of 853 $m^2\ g^{-1}$ after extraction of the amine template with a dilute solution of nitric acid, but again, the structure completely collapsed upon phase transformation. Very recently, Tatsumi et al.[23] developed a very efficient procedure to prepare template-free mesostructured titania with crystallized walls. After the complete extraction of the amine-surfactant with *p*-toluenesulfonic acid, the template-free sample is exposed to titanium tetraisopropoxide by chemical vapor deposition, followed by a treatment with water vapor to decompose the deposited titanium alkoxide. The CVD procedure stabilized the pure titania mesostructure creating crystallinity on the surface without the need of high-temperature treatment. The CVD-stabilized samples have an improved thermal stability in terms of time (at 300 °C), but there is no mention of higher stability in terms of temperature.

Up to now, most reports involving mesostructured titania have emphasized the control of the different processes occurring during synthesis and the removal of the template to create a stable template-free titania mesophase. After removal of the template by thermal decomposition or extraction, the walls of these mesostructured phases are composed of pure amorphous titania or amorphous titania with a small amount of crystalline anatase nanobuilding blocks. However, a further thermal treatment to transform the walls from amorphous titania to the more desirable anatase crystal phase results in a total collapse of the pore system.

As most reports have focused on methods to control the indiscriminate polymerization of the titania source before mesostructure formation, we developed a new synthesis step that controls the transformation of the amorphous titania walls of surfactant-assembled titania into crystalline walls.

Experimental Section

Synthesis. For the syntheses of mesoporous titania, amine templates, in particular hexadecylamine (HA; Acros 90%) and *N*,*N*-dimethylhexadecylamine (NNHA; Fluka >95%) and cetyl trimethylammonium bromide (CTABr; Acros 99%), were used while titanium tetra-isopropoxide ($Ti(O^iPr)_4$; Aldrich 97%) was used as titanium source.

Evaporation-Induced Self-Assembly (EISA). In a typical amine-templated synthesis, the amine was dissolved in ethanol (Merck; absolute grade). To this solution, the titanium tetra-isopropoxide was added and stirred at ambient temperature. After a dropwise addition of water to this mixture, a white suspension was formed and the solution was stirred for 15 min. Additionally, the solution was aged at room temperature in a closed system to avoid evaporation. The molar gel composition was Ti/amine/H_2O/ethanol = 1/0.33/2/90. After 24 h aging, the mixture was transferred into a Petri dish to evaporate the solvent in open air at room temperature. Titania mesostructures synthesized by this EISA technique are further named as Ti−HA−EISA or Ti−NNHA−EISA, where HA and NNHA stand for mesophases prepared with hexadexylamine and *N*,*N*-dimethylhexadecylamine, respectively.

According to the synthesis of Sanchez et al.,[19] the EISA-procedure was also used to prepare CTABr-templated titania hybrid as follows: Ti−CTABr was synthesized by the addition of titanium isopropoxide ($Ti(O^iPr)_4$) to an ethanolic HCl (Acros pro analysis grade) solution. An ethanolic solution of CTABr was added and the hybrid was formed in an open Petri dish at 60 °C for 7 days. The molar ratios were Ti:CTABr:HCl:H_2O:EtOH = 1:0.16:1.4:17:20. Titania hybrids synthesized by this procedure are further denoted as Ti−CTABr−EISA.

NH_3-Treatment. NH_3-treatment was carried out in a reflux system. NH_4OH (Merck 25% p.a.) was added to pure water until a pH of 9 to 10 was reached. For the amine-templated samples, a part of the mixture after aging for 24 h before evaporation of the solvent was filtered and the wet solid was added to the water and the pH was again brought to a value between 9 and 10. For 1 g of wet solid, 50 mL of basic water was used. The solution was refluxed for 48 h and the pH was kept between a value of 9 and 10. Amine-titania hybrids synthesized by this procedure are further denoted as Ti−HA−NH_3 or Ti−NNHA−NH_3. For CTABr-titania, a part of the aged sample is used to reflux in ammonia in exactly the same way as for the amine-assembled titania. These samples are further denoted as Ti−CTABr−NH_3.

Characterization. X-ray diffractogram patterns were recorded on a Philips PW1840 powder diffractometer, using Ni-filtered Cu Kα radiation. Porosity and surface area studies were performed on a Quantachrome Autosorb-1-MP automated gas adsorption system. All samples were outgassed for 16 h at 200 °C prior to adsorption. Gas adsorption occurred using nitrogen as the adsorbate at liquid nitrogen temperature (77 K). The SEM image was recorded using a JEOL-JSM-6300 scanning electron microscope operating at an accelerating voltage of 20−30 kV. The sample was sputtered with a thin film of gold. TEM images were recorded by using a Philips CM12 microscope. Powder samples were deposited onto a copper mesh grid coated with a carbon film. A Nicolet Nexus 670 bench equipped with a Ge detector was used for Raman spectroscopy. Samples were measured in a home-built in situ spectroscopic cell for Fourier transform Raman, which can be vertically attached to the baseplate of the Nexus instrument. The in situ cell is designed with a cylindrical furnace, controlled by a temperature controller (Eurotherm), containing a quartz sample tube that is connected to the inlet and outlet of a gas flow setup. The laser beam is focused onto the sample through a window in the stainless cover and the cylindrical furnace. Samples were measured in a 180° reflective sampling configuration using a 1064 nm Nd:YAG laser. Five hundred scans were averaged for each spectrum. Samples were heated at a heating rate of 5 °C min^{-1} under a flow of pressed air at a flow rate of 50 $cm^3\ min^{-1}$. Spectra were recorded in steps of 50 °C. The thermogravimetric analysis (TGA) experiments and the differential scanning calorimetric measurements (DSC) were performed on an SDT2960 module (TA-instruments). Samples were heated at a heating rate of 5 °C min^{-1} under a N_2 atmosphere (TGA and DSC) or a flow of pressed air (TGA) at a flow rate of 50 $cm^3\ min^{-1}$.

Thermal Stability. To assess thermal stability, the samples were calcined in air starting from an end-temperature of 300

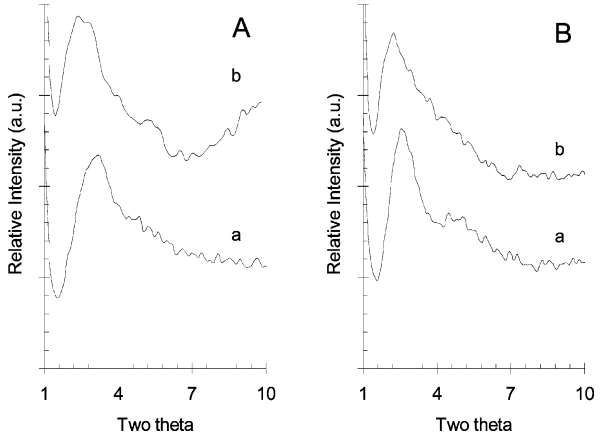

Figure 1. Powder X-ray diffraction patterns of Ti−EISA (A) and Ti−NH_3 (B) prepared with HA (a) and NNHA (b).

°C. The end-temperature was each time increased with 100 °C as long as no complete collapse of the titania mesostructure had occurred. All the sample precursors were calcined with a heating rate of 2 °C min^{-1} and kept at the end temperature for 2 h.

Results and Discussion

a. Synthesis of Amine-Hybrid Phases. In previously published data reported on amine-assembled titania-based mesostructures, the mesophase formation and the high reactivity of the titanium alkoxide was controlled by applying an aging procedure in acidic conditions[23] or by using ultrasonic waves[21,22] which in both cases eliminate the restrictions on the amount of water during syntheses. To control the reactivity of the titanium source and mesostructure formation, we used an aging procedure that is very similar to the acidified aging method, yet only very small quantities of water are being used instead of an acid. Two major steps are being separated during this aging procedure. In a first step, hexadecylamine or *N*,*N*-dimethyl hexadecylamine was dissolved in absolute ethanol followed by the addition of titanium isopropoxide ($Ti(O^iPr)_4$). Similar to the synthesis of mesoporous titania with block copolymer templates described by Stucky et al.,[24] the formation of rodlike micelles takes place by a mechanism that combines amine self-assembly with complexation of these amines with the titanium alkoxide. In the second step, a very low quantity of water with a molar ratio $Ti/H_2O = 1/2$ is slowly added avoiding the formation of a dense poorly structured inorganic network, yet leading to the formation of a low-condensed titania−amine complex micellar system. After this aging procedure, two different strategies are applied to extend further hydrolysis and polymerization of the low-condensed titania walls into the final amine−titania hybrids. In the first pathway, we make use of the so-called evaporation-induced self-assembly (EISA) technique, which is successfully applied to the syntheses of mesoporous titania with poly(ethylene)-based[26] or quaternary ammonium bromide surfactants.[19] The amine−titania hybrid formation and the inorganic polymerization of the titania walls are continued during a solvent evaporation process in open air in combination with the uptake of water provided by moisture in the air. The second route that has been followed is also a completely new method for the synthesis of mesostuctured titania where the aged product is transferred into an excess of water containing ammonia.

The X-ray diffraction patterns of titania samples prepared with hexadecylamine and *N*,*N*-dimethyl hexadecylamine are shown in Figure 1A and B, respectively, for both synthesis pathways. The Ti−HA−EISA and Ti−HA−NH_3 samples both exhibit a single-first-order reflection in the X-ray diffraction pattern in the 2θ range 2−4 corresponding to a pore center to pore center correlation length. This degree of ordering indicates that mesostructured titania-hybrids are well formed in both synthesis pathways. Furthermore, the X-ray diffraction patterns are very similar to previously reported data on mesoporous titania hybrids prepared with primary amines.[21−23] As expected, a comparable diffraction behavior can be observed for the titania hybrids prepared with NNHA since this template is very similar to hexadecylamine.

b. Thermal Analysis. Several techniques such as XRD, N_2-adsorption−desorption, in situ Raman spectroscopy, TGA, and DSC were used to gain insight in the processes occurring during thermal treatment of the different titania mesophases as well as the consequences on their thermal stability. Figure 2A and B shows X-ray diffractograms as a function of calcination temperature of Ti−HA−EISA and Ti−HA−NH_3 samples, respectively. A clear retention of the diffraction line can be observed for both mesophases up to a calcination temperature of 350 °C. When samples are further calcined at 400 °C, the diffraction peak can still be seen for the Ti−HA−NH_3 sample whereas in Ti−HA−EISA, the reflection totally disappears indicating a degradation of the mesopore structure. Moreover, a single peak appears at $2\theta = 25.5°$ which is assigned to the crystalline anatase phase of titania.[31] By using the width of the anatase diffraction peak and the Scherrer equation, the average crystal grain size is estimated to have a value of 16.9 nm. On the basis of similar diffraction observations, even an average crystal grain size of 45.5 nm can be estimated for Ti−NNHA−EISA. The results obtained from X-ray diffraction measurements are in agreement with Figure 3, presenting the N_2-adsorption−desorption isotherms of Ti−EISA and Ti−NH_3 samples calcined at 300 and 400 °C for 2 h. The physical characteristics are summarized in Table 1. For both titania materials calcined at 300 °C for 2 h, the N_2-isotherms show high porosity properties having BET surface areas around 400 $m^2\ g^{-1}$ and mesopore volumes of almost 0.2 $cm^3\ g^{-1}$. However, a further subjection of Ti−HA−EISA to a temperature of 400 °C for 2 h yields a surface area of merely 5 $m^2\ g^{-1}$ and no mesopore volume remains. Under these conditions, Ti−HA−NH_3 still features a surface area and mesopore volume of 291 $m^2\ g^{-1}$ and 0.16 $cm^3\ g^{-1}$, respectively. From Table 1, one can observe a similar behavior for the titania samples prepared with *N*,*N*-dimethyl hexadecylamine. On the basis of the above observations, titania hybrids prepared by the EISA pathway totally collapse above 350 °C by the extensive growth of anatase crystallites, whereas despite a shrinkage in pore volume and BET surface area, the mesoporous network remains intact in the NH_3 strategy.

Compared to X-ray diffraction, Raman spectroscopy is a much more sensitive technique for the detection of nanosized crystalline domains. To get more insight in the local crystal structures formed during thermal treatment, Figure 4 represents the in situ Raman spectra of the Ti−HA samples measured in steps of 50 °C under a flow of air. The Ti−HA−EISA material does not display any peaks up to 350 °C. In accordance with the X-ray diffractogram, three clear bands at 399, 519, and 638 cm^{-1}, characteristic for anatase,[31] appear at a calcination temperature of 400 °C. For the sample treated with NH_3, two lines at 442 and 611 cm^{-1} emerge at 200 °C. These Raman bands, ascribed to the rutile crystal phase,[31] are observed in the in situ spectra up to a temperature of 300 °C. Upon further increase of the calcination temperature to 350 °C, additional Raman lines appear at 399, 519, and 638 cm^{-1} which are characteristic for the anatase phase. The two bands characteristic

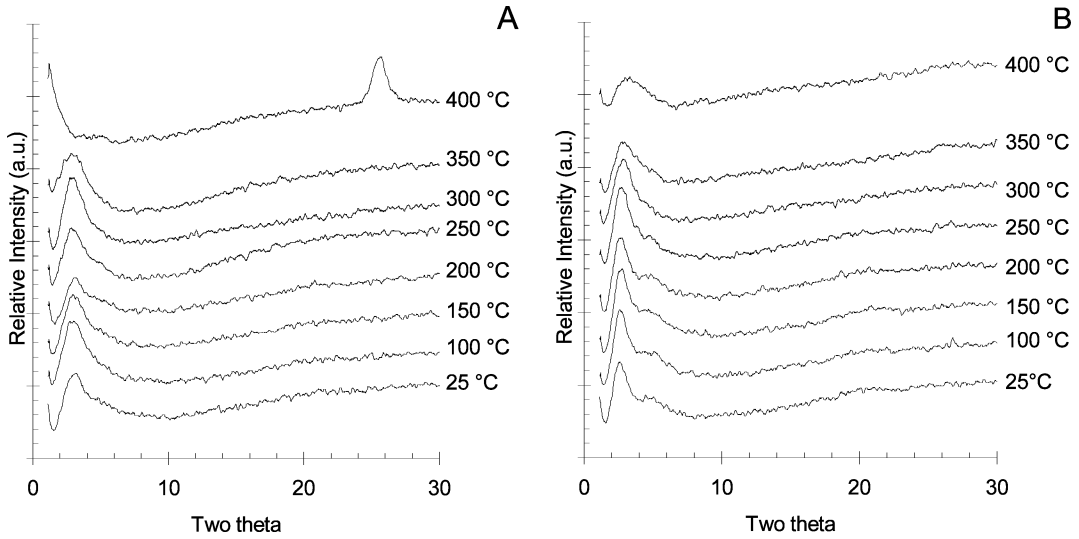

Figure 2. Powder X-ray diffraction patterns of Ti−HA−EISA (A) and Ti−HA−NH_3 (B) as a function of calcination temperature.

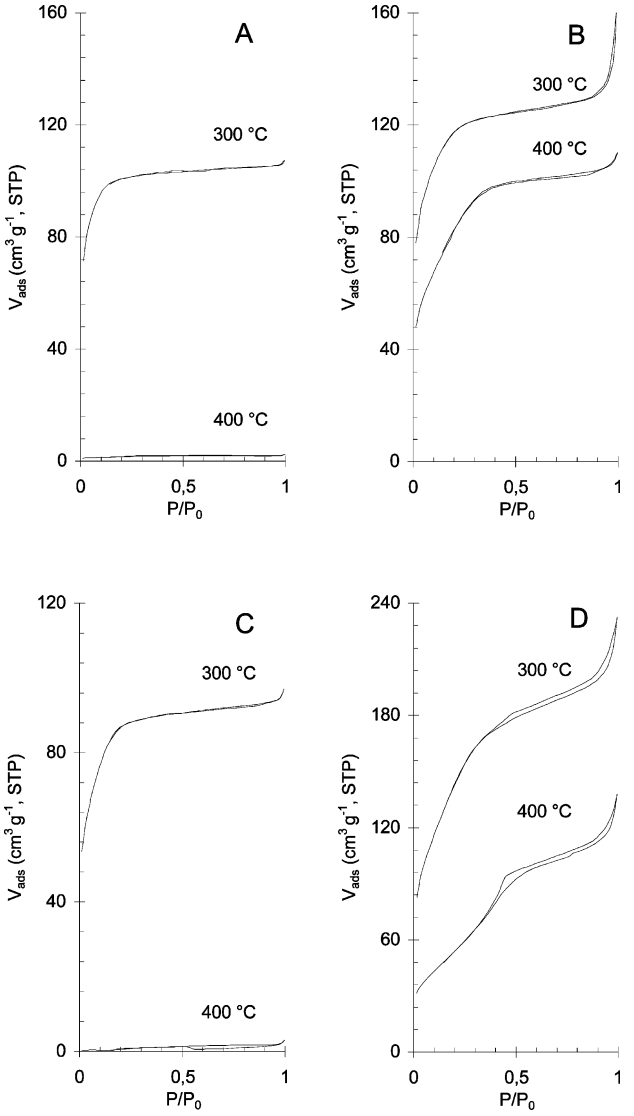

Figure 3. N_2 adsorption−desorption isotherms of Ti−HA−EISA (A), Ti−HA−NH_3 (B), Ti−NNHA−EISA (C) and Ti−NNHA−NH_3 (D) calcined at 300 and 400 °C for 2 h.

for the rutile phase are still present at 350 °C, but these bands are relatively hard to observe in Figure 4B because the lines related to anatase are relatively dominant. This is further illustrated by the enlargement of the Raman spectrum of samples heated to 300 (rutile) and 350 °C (Figure 4C). The latter spectrum still shows a clear rutile band at 442 cm^{-1}, while the shoulder of the anatase peak with maximum at 638 cm^{-1} is caused by the underlying rutile band at 611 cm^{-1}. This observation is not unexpected since rutile is the thermodynamically stable polymorph, whereas anatase is a kinetic, metastable product. Therefore, the rutile nanoparticles should still be present because these particles can only be "irreversibly" formed. DSC and TGA measurements shown in Figure 5 further confirm these observations. The DSC patterns display two corresponding calorimetric processes for both synthesis procedures. The different stages can be described as follows: A clear endothermic peak in the range of 25−120 °C (peak a) is attributed to the elimination of water and ethanol and is associated with a weight loss of around 10% in the TGA curves. From 250 to 400 °C (peak b), a broad exothermic process can be observed. This broad exothermic process is probably caused by two contributions: In combination with the TGA curve, a mass loss of 30% can be observed in this temperature range, which is attributed to the decomposition of the template. In combination with the Raman spectra for both Ti−HA−EISA and Ti−HA−NH_3, a second contribution is caused by the exothermic crystallization of amorphous titania into anatase crystallites. Despite the similarity in the DSC patterns for both titania syntheses, a closer look to the DSC curve of Ti−HA−NH_3 reveals an additional relative small exothermic process between 130 and 180 °C with a maximum at 160 °C (peak c) that does not take place in Ti−HA−EISA. No mass losses are observed in the TGA curve in this temperature range. This additional exothermic process can be attributed to the crystallization of some amounts of amorphous TiO_2 to rutile, as evidenced by the appearance of rutile bands in the in situ Raman spectra between 150 and 200 °C.

TEM images support the XRD, Raman, and DSC information. Figure 6 shows TEM images of the Ti−HA−NH_3 sample calcined at 300 °C. A selected area electron diffraction pattern of Ti−HA−NH_3 calcined at 300 °C (Figure 6A) confirms the formation of rutile nanoparticles. Four rutile rings can be observed, in particular, (from small to large rings) indexed as 110 (d = 3.24), 210 (d = 2.05), 211 (d = 1.69), and 321 (d = 1.17).

According to the results above, the thermal processes occurring in the conventional EISA synthesized titania mesophases are different compared to the innovative NH_3-treated titania

TABLE 1: Physical Characteristics of Ti−EISA and Ti−NH_3 Samples

sample	calcd temp (°C)	S_{BET} (m^2 g^{-1})	d (Å)	D_{BJH} (Å)	V_p (cm^3 g^{-1})	crystal phase
Ti−HA−EISA	noncalcined		28.4			amorphous
	300	393	28.7	*b*	0.16	amorphous
	400	5	*c*	*a*	*a*	anatase
Ti−NNHA−EISA	noncalcined		36.3			amorphous
	300	329	37.2	14.9	0.29	amorphous
	400	5	*c*	*a*	*a*	anatase
Ti−HA−NH_3	noncalcined		34.6			amorphous
	300	435	29.7	*b*	0.19	amorphous + rutile
	400	291	47.2	19.6	0.16	anatase + rutile
	500	123	48.7	20.7	0.08	anatase + rutile
	600	52	*c*	21.5	0.03	anatase + rutile
Ti−NNHA−NH_3	noncalcined		39.6			amorphous
	300	508	34.3	18.0	0.29	amorphous + rutile
	400	192	51.0	34.3	0.16	anatase + rutile
	500	142	52.2	35.9	0.12	anatase + rutile
	600	94	*c*	34.2	0.10	anatase + rutile

[a] No capillary condensation step was observed in the N_2 isotherm. [b] The pores are too small. [c] No diffraction peak was observed or the peak was too broad to determine the position.

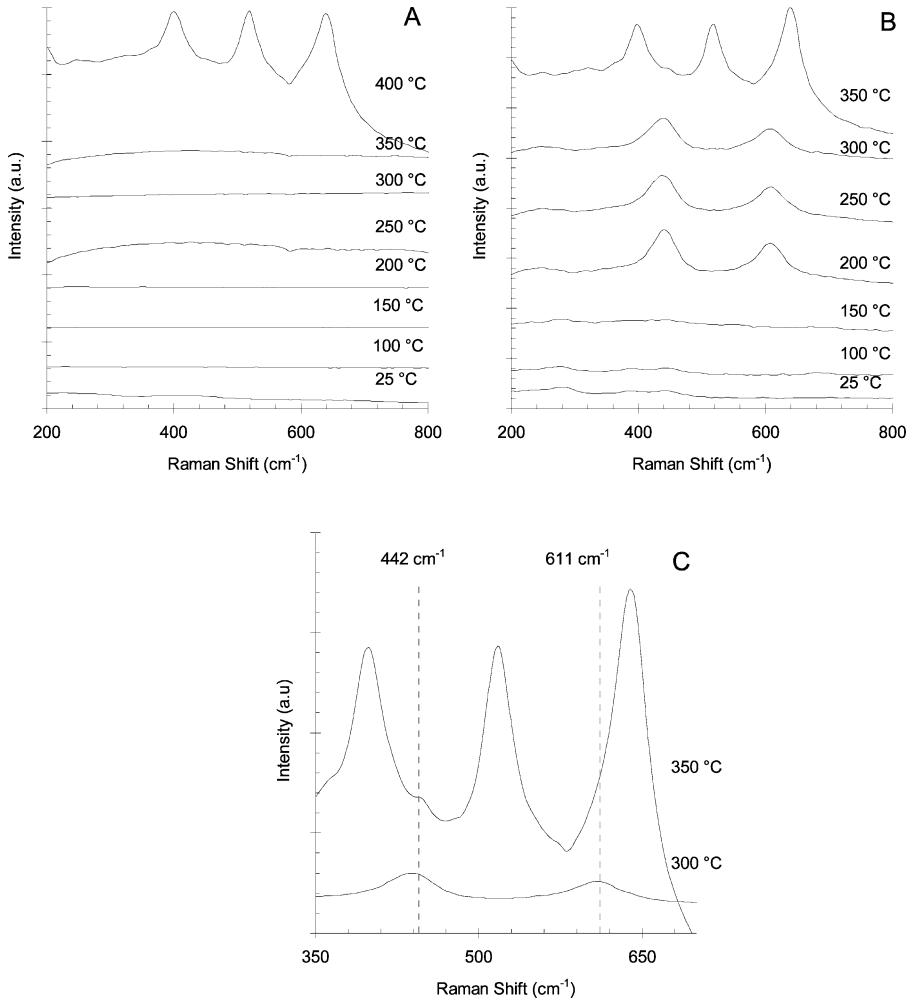

Figure 4. In situ Raman spectra of Ti−HA−EISA (A) and Ti−HA−NH_3 (B and C) as a function of calcination temperature.

hybrids. In the EISA-samples, the calcination path from hybrid precursor to template-free titanium oxide can be divided into three stages and can further be described as follows: (a) After synthesis, the amine−titania hybrid consists of amorphous titania walls. On the basis of TGA-measurements in air (not shown), the combustion of the amine-template is the first process occurring at a temperature of 210 °C. (b) Second, after a further increment to a temperature of 350 °C, an amine-free mesostructure with an array of amorphous TiO_2 is formed. (c) The amorphous titania walls are further transformed into anatase between 350 and 400 °C. This crystallographic reorganization takes place in the absence of template and no medium is available to "freeze" or "block" the nuclei growth. As a consequence, the nanobuilding blocks have a free hand in the uncontrolled growing to robust anatase crystals, and thus the mesoporous amorphous titania is transformed into a nonporous anatase crystal phase with grain sizes with an average size that is much larger than the dimension of the original pores.

In contrast, the calcination of NH_3-treated samples occurs in a much more controlled way by means of an additional step.

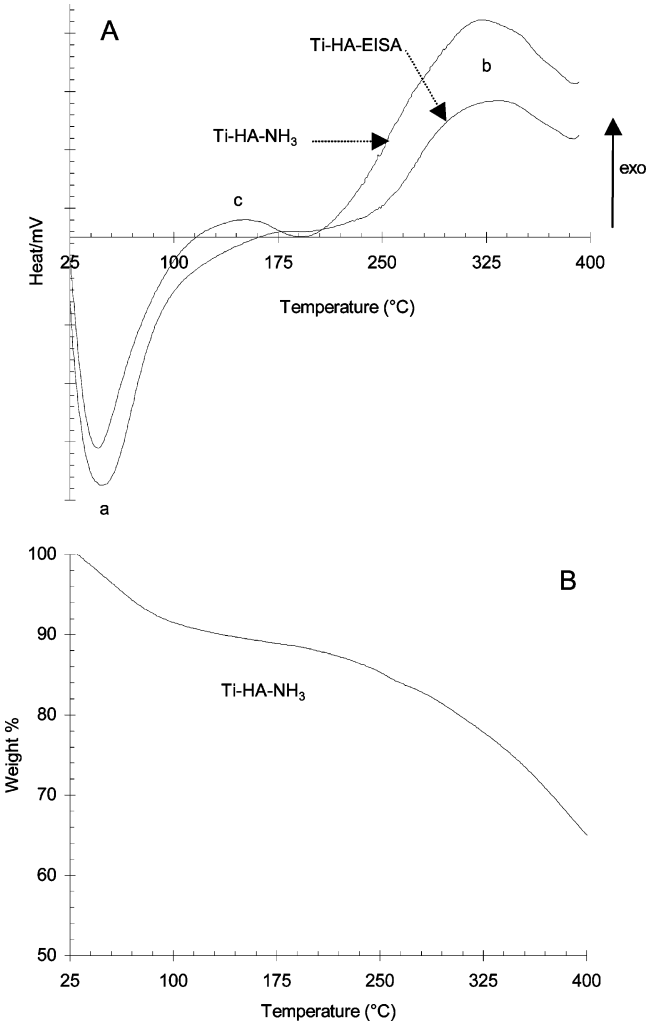

Figure 5. DSC curves of Ti−HA−EISA and Ti−HA−NH_3 (A) and TGA curve (N_2) of Ti−HA−NH_3 (B).

During the refluxing of titania hybrids in NH_4OH, ammonia is slowly entering the pore channels. We suggest that NH_3 interacts with residual Ti−OH groups. Promoted by the NH_3, the parts of the amorphous titania walls of the titania hybrids are transformed into rutile nanobuilding blocks between 150 and 200 °C, thus before thermal removal of the template. This observation is similar to the results observed by Lewis et al.,[32] who prepared pure "rutile" crystals by hydrolysis of $TiCl_4$ with NH_4OH followed by a similar heat treatment. Furthermore, Jung et al.[33] also observed the formation of rutile crystallites in the amorphous matrix of TiO_2 films promoted by interaction with NH_3. The micellar templates, which are still in the structure at this temperature, preserve the meso-organized network and only the amorphous particles, which were in interaction with NH_3, will be promoted to transform into rutile nanoparticles. The meso-organized walls are from now on built up of amorphous titania, incorporated with some random distributed nanosized rutile crystallites. Upon further heating to 300 °C, the template is burned out of the rutile-incorporated hybrid. The rutile particles do not grow upon this temperature increment. This is further confirmed by the absence of characteristic rutile reflections in the XRD-pattern (Figure 2B) of the Ti−NH_3 samples calcined at 300 °C, indicating that the rutile crystals are too small to be detectable by XRD. By a subsequent increase of temperature, a transformation from the residual amorphous particles to metastable anatase occurs. This crystallization process is accompanied by a retention of the pore structure as

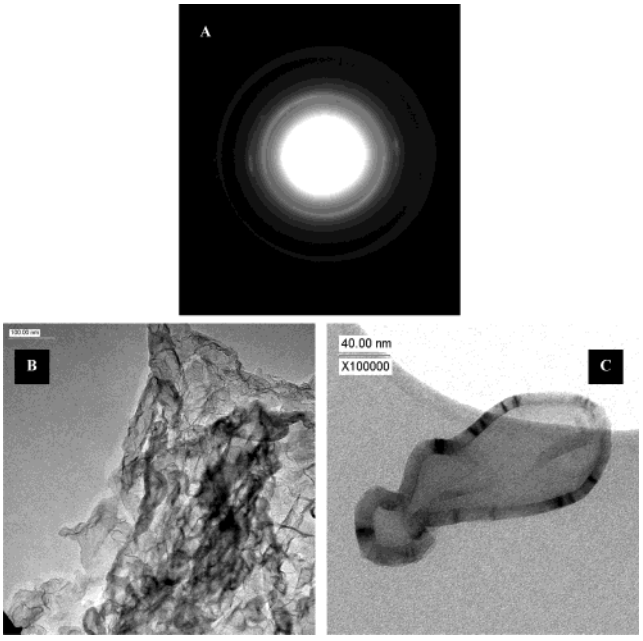

Figure 6. Representative TEM micrographs of Ti−HA−NH_3 calcined at 300 °C. (A) Selected area electron diffraction rings of rutile, (B) overview image at low magnification, and (C) image at high magnification.

still a clear diffraction peak can be observed in the low angle range (Figure 2). In contrast to EISA samples thermally treated at 400 °C, no anatase peak appears in the X-ray diffractogram which, together with the preservation of the porosity characteristics, indicates that the formation of the anatase particles was carefully performed. One can suspect that extended crystallization from the residual amorphous titania to robust large anatase grains is avoided by the presence of incorporated rutile nanobuilding blocks in the walls. The individual residual amorphous particles are separated by stable rutile nanosized particles in such a way that, after transformation to anatase, the growth of these formed anatase particles is blocked by the presented rutile species.

c. General Features of Synthesized Amine-Assembled Titania Samples. As already mentioned above, calcination of both Ti−EISA and Ti−NH_3 samples at 300 °C leads to pore structures with high surface areas and pore volumes up to 508 $m^2\ g^{-1}$ and 0.29 $cm^3\ g^{-1}$, respectively, as further summarized in Table 1. However, despite these high porosity properties, the calcination is not completely terminated because of residual carbonaceous material in the pores (black-colored samples). This can also be seen in the N_2-adsorption−desorption isotherms of titania samples calcined at 300 °C (Figure 3) showing pores in the micro-mesopore range having BJH pore diameters of 18 Å or smaller. The residual organic material partially blocks the pores and reduces the pore diameter. Therefore, despite the total collapse of Ti−EISA samples upon extended anatase formation at 400 °C, a thermal treatment to 400 °C in the Ti−NH_3 samples renders organic-free structures with diameters shifted to the mesopore range. From results described above, one could observe that the Ti−HA samples follow the same trend as Ti−NNHA materials, which is not surprising because of their large similarity. However, a more detailed look to the N_2-adsorption−desorption isotherms (Figure 3) together with their physical data (Table 1) reveals that the pore diameters and *d*-spacings are larger in Ti−NNHA. After calcination at 400 °C, the BJH pore diameters of Ti−NNHA−NH_3 and Ti−HA−NH_3 are 34.3 and 19.6 Å, respectively, whereas the *d*-values of both samples are

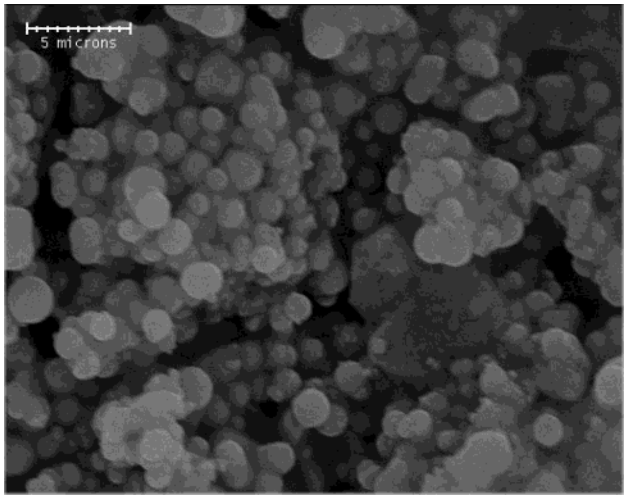

Figure 7. Representative scanning electron microscopy (SEM) image of Ti−HA−NH_3.

51.0 and 47.2 Å, respectively. This difference can be explained by the larger surfactant headgroup of *N*,*N*-dimethylhexadexylamine.

All of the titania mesostructures synthesized in this work exhibit a single-first-order reflection which is consistent with the XRD patterns of similar mesostructures prepared with amines reported in the literature, for example, mesoporous titania[21−23] and hexagonal mesoporous silica assembled in neutral[34] and acidic medium.[35] Moreover, the amine templates direct all these mesostructures into a wormhole-like ordering. Furthermore, the shape of the isotherms and the derived pore size distributions (relatively broad low-intensity peaks) of samples reported in this paper are in very good agreement with the amine−titanias prepared by Gedanken et al.[21,22] and Tatsumi et al.,[23] also having BET surfaces and pore volumes of around 450 $m^2\ g^{-1}$ and 0.3 $cm^3\ g^{-1}$, respectively, when calcined at 300 or 350 °C. One can therefore claim that the titania samples prepared in this report also exhibit a wormhole-like structure. Moreover, the SEM micrograph in Figure 7 shows that the Ti−HA−NH_3 sample calcined at 400 °C consists of spherical particles with an average size of 1 to 2 μm, which was also observed for the wormhole-like amine-templated titania of Tatsumi et al. Furthermore, an overview image at low magnification (Figure 6B) illustrates that the Ti−HA−NH_3 material is almost exclusively composed of folded foils without the formation of large agglomerates. An image at high magnification (Figure 6C) of Ti−HA−NH_3 clearly shows that the foils are composed of discrete nanoparticles.

d. Thermal Stability. Most work dealing with the synthesis of mesostructured titania reported a limited thermal stability to a maximum temperature of 350 °C. Above 350 °C, stability limitations arise by the massive formation of pure anatase from amorphous titanium dioxide which was also observed for the samples prepared by the EISA procedure. In contrast, XRD and N_2-sorption data showed that the mesoscale order is at least kept until a 2-h treatment at 400 °C for titania samples treated with NH_3. To assess the absolute upper limit of the thermal stability, Ti−HA−NH_3 and Ti−NNHA−NH_3 samples were heated at various temperatures for 2 h. Figures 8 and 9 display the changes in XRD patterns and N_2-adsorption−desorption isotherms, respectively, starting from a calcination temperature of 400 °C. The physical parameters in Table 1 indicate that the pore volume and specific surface area decrease as a function of temperature. This can be explained by the further segregation and growth of anatase nanobuilding blocks from the mesostructure to form nonporous massive anatase grains. This is further confirmed by the appearance of an anatase peak in both X-ray diffraction patterns at $2\theta = 25.5°$ from 500 °C (not shown). However, a large part of the mesoscale order is conserved as both Ti−NH_3 samples exhibit isotherms with a well-developed capillary condensation step up to a temperature of 600 °C, whereas the powder X-ray diffraction patterns show retention of the low-angle diffraction peak to at least 500 °C. Furthermore, surface areas and pore volumes from around 130 $m^2\ g^{-1}$ and 0.10 $cm^3\ g^{-1}$, respectively, can be observed after thermal treatment at 500 °C.

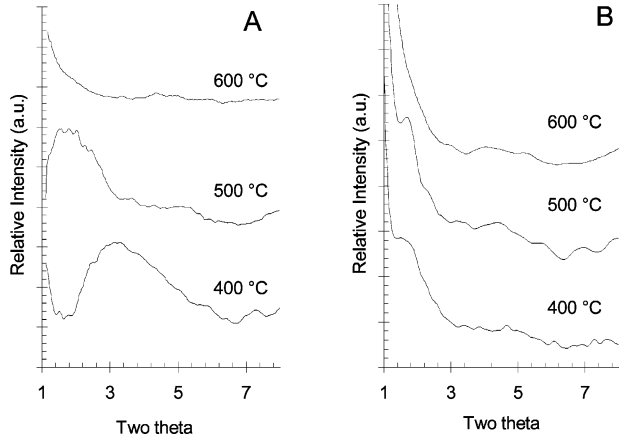

Figure 8. Powder X-ray diffraction patterns of Ti−HA−NH_3 (A) and Ti−NNHA−NH_3 (B) calcined at 400, 500, and 600 °C.

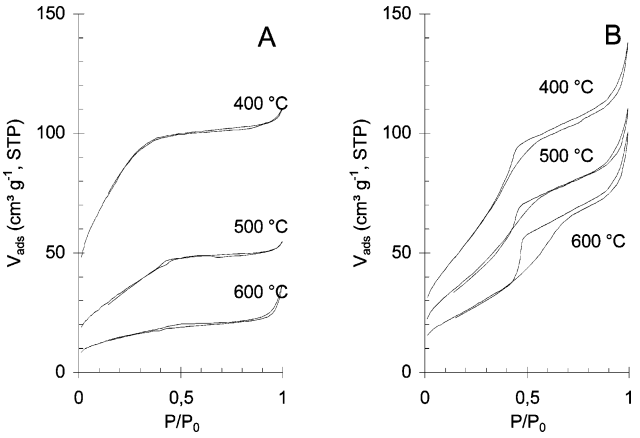

Figure 9. N_2 adsorption−desorption isotherms of Ti−HA−NH_3 (A) and Ti−NNHA−NH_3 (B) calcined at 400, 500, and 600 °C.

The observations above demonstrate that the controlled generation of rutile nanobuilding blocks into the amorphous walls of titania hybrids before the removal of the template has a beneficial influence on the thermal stability. The extended sintering process from anatase is shifted from 350 °C for Ti−EISA samples and other mesoporous titanias reported in the literature to temperatures higher than 500 °C for NH_3-treated samples.

e. Extension to CTABr-Templated Mesostructured Titania. Since NH_3 interacts with the amorphous walls of the hybrid, the post-treatment should also be extendable to hybrids directed by other templates. To verify whether this stabilization procedure is indeed generally applicable to all hybrids consisting of amorphous titania walls, a recently described synthesis toward titania directed with CTABr has been chosen.[19]

The shape of the N_2 isotherms (Figure 10A) and XRD-patterns (Figure 10B) of Ti−CTABr−NH_3 samples are very similar to those of Ti−CTABr−EISA in the original report of

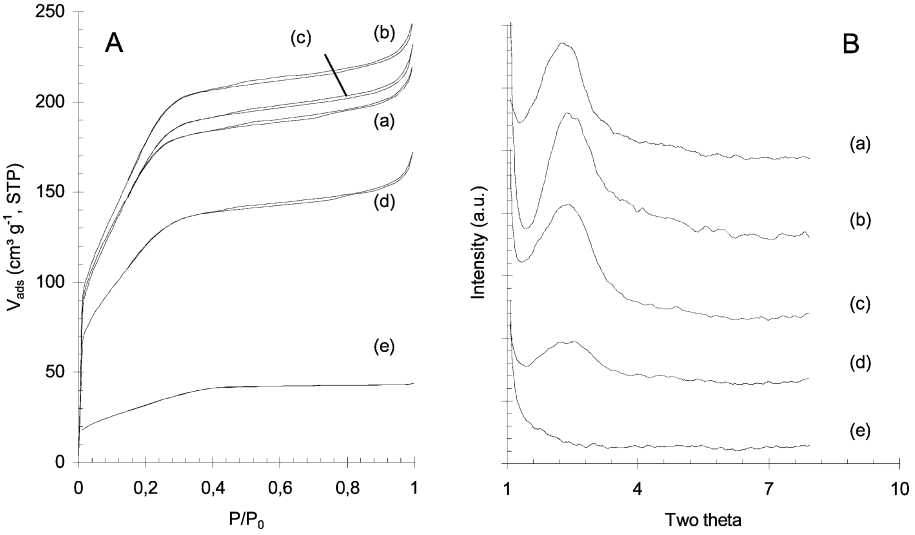

Figure 10. N_2 adsorption−desorption isotherms (A) and XRD patterns (B) of Ti−CTABr−NH_3 samples calcined at (a) 300 °C, (b) 400 °C, (c) 500 °C, (d) 600 °C for 2 h and (e) Ti−CTABr−EISA calcined at 400 °C for 2 h.

TABLE 2: Physical Characteristics of Ti−CTABr-EISA and Ti−CTABr−NH_3 Samples Calcined at Different Temperatures

sample	calcd temp (°C)	S_{BET} (m^2 g^{-1})	D_{BJH} (Å)	V_p (cm^3 g^{-1})	crystal phase
Ti−CTABr−EISA	300	466	*a*	0.19	amorphous
	400	112	*b*	0.06	anatase
	500	8	*b*	*b*	anatase
Ti−CTABr−NH_3	300	585	18.5	0.28	amorphous + rutile
	400	613	19.0	0.32	anatase + rutile
	500	576	18.9	0.29	anatase + rutile
	600	420	18.6	0.21	anatase + rutile

[a] The pores are too small to use the BJH method. [b] No mesoporosity is observed.

Sanchez et al.[19] To compare the EISA and NH_3-synthesized samples, the upper limits of their thermal stability were explored by heating the samples at various temperatures for 2 h starting from a calcination temperature of 300 °C.

Similar to amine-templated titania prepared by the EISA-procedure, the Ti−CTABr−EISA sample is totally destroyed upon calcination at 400 °C. In contrast, a large part of the mesoscale order is conserved as Ti−CTABr−NH_3 exhibits isotherms with a well-developed capillary condensation step and a clear d_{100}-reflection up to a temperature of at least 600 °C. These observations are further supported by the physical data provided in Table 2. Ti−CTAB−NH_3 retains more than 65% of its initial surface area and framework pore volume at 600 °C. This study illustrated that the simple NH_3-treatment can be successfully extended to other surfactant-assembled materials.

Conclusions

Mesoporous wormhole-like titania was prepared by applying a hexadecylamine and *N*,*N*-dimethylhexadecylamine templating method. As most reports in the literature have focused on methods to control the indiscriminate polymerization of the titania source before mesostructure formation, we have emphasized on the controlled transformation of the amorphous titania walls into crystalline anatase. This phase transformation was very critical: by calcination of titania hybrids up to a temperature of 400 °C to remove the templates, the whole mesostructure was completely destroyed by the extensive growth of anatase grains.

By a simple additional synthesis step presented in this work, aged titania precursors were treated with aqueous ammonia yielding amine−titania hybrids with similar characteristics as the titania hybrids, prepared by the commonly used evaporation-induced self-assembly (EISA) technique. We found that, during thermal treatment, the ammonia adsorbed in the pore channels promotes the transformation of some amorphous titania particles into thermodynamically stable nanosized rutile crystallites before the template was burned out of the mesostructure. The walls of the hybrid composite consist from now on of amorphous titania incorporated with rutile nanodomains. After a subsequent increase of temperature to remove the template, the resulting amorphous particles were transformed into anatase in such a way that this crystallographic transformation is accompanied by a retention of the pore structure. The preformed rutile particles limited the particle growth of the formed anatase nanobuilding blocks, thereby yielding a template-free high surface area titania mesostructure built up of walls consisting of rutile and anatase nanobuilding blocks. Moreover, these pure mesoporous titanias prepared by the NH_3-pathway exhibited an outstanding thermal stability to at least 500 °C, whereas the titania samples prepared by the EISA-procedure completely collapsed at a calcination temperature of 350 °C.

Finally, it was illustrated that the NH_3-treatment can be successfully extended to other surfactant-assembled titania materials, for example, the thermal stability of titania prepared with CTABr is increased from 300 °C to 600 °C. This successful method opens a new area in the synthesis and applications of titania materials.

Acknowledgment. This work was sponsored by a grant of the F.W.O.-Vlaanderen (Fund for Scientific Research, Flanders, Belgium), Grant Number G.0446.99. P.C. thanks the F.W.O.-Flanders for a position as senior research assistant. T.L. is indebted to the IWT-Flanders-Belgium for a Ph.D. grant. The authors wish to thank Prof. H. Desseyn and Mr. J. Janssens for the DSC and TGA measurements.

References and Notes

(1) Kresge, C. T.; Leonowics, M. E.; Roth; W. J.; Vartulli, J. C.; Beck, J. S. *Nature* **1992**, *359*, 710.

(2) Beck, J. S.; Vartuli, J. C.; Roth, W. J.; Leonowics, M. E.; Kresge, C. T.; Schmitt, K. D.; Chu, C. T.-W.; Olson, D. H.; Sheppard, E. W.; McCullen, S. B.; Higgings, J. B.; Schlenker, J. L. *J. Am. Chem. Soc.* **1992**, *114*, 10834.

(3) Reviews on this subject including (a) Ciesla, U.; Schuth F. *Microporous Mesoporous Mater*. **1999**, *27*, 131. (b) Barton, T. J.; Bull, L. M.; Klemperer, W. G.; Loy, D. A.; McEnaney, B.; Misono, M.; Monson, P. A.; Pez, G.; Scherer G. W.; Vartuli, J. C.; Yaghi, O. M. *Chem. Mater*. **1999**, *11*, 2633. (c) Oye, G.; Sjoblom, J.; Stocker, M. *Adv. Colloid Interface Sci.* **2001**, *89*, 439. (d) On, D. T.; Desplantier-Giscard, D.; Danumah, C.; Kaliaguine, S. *Appl. Catal., A* **2001**, *222*, 299. (e) Linssen, T.; Cassiers, K.; Cool, P. *Adv. Colloid Interface Sci.* **2003**, *103*, 121.

(4) Pelizzetti, E.; Minero, C.; Borgarello, E., Tinucci, L.; Serpone, N. *Langmuir* **1993**, *13*, 2995.

(5) Ohtani, B.; Ogawa, Y.; Nishimoto, S. *J. Phys. Chem. B* **1997**, *101*, 3746.

(6) Rivera, A. P.; Tanaka, K.; Hisanaga, T. *Appl. Catal., B* **1993**, *3*, 37.

(7) O'Regan, B.; Grätzel, B. M. *Nature* **1991**, *352*, 737.

(8) Nazeeruddin, M. K.; Kay, A.; Rodicio, L.; Humphry-Baker, R.; Müler, E.; Liska, P.; Vlachopoulos, N.; Grätzel, M. *J. Am. Chem. Soc.* **1993**, *115*, 6382.

(9) Luo, S. C.; Ollos, D. F. *J. Catal*. **1996**, *163*, 1.

(10) Cao, L. X.; Huang, A. M.; Spiess, F.-J.; Suib, S. L. *J. Catal.* **1999**, *188*, 48.

(11) Luo, S. C.; Falconer, J. L. *J. Catal.* **1999**, *185*, 393.

(12) Cao, L. X.; Gao, Z.; Suib, S. L.; Obee, T. N.; Hay, S. O.; Freihaut, J. D. *J. Catal.* **2000**, *196*, 253.

(13) Hoffmann, M. R.; Martin, S. T.; Choi, W.; Bahnemann, D. W. *Chem. Rev*. **1995**, *95*, 69.

(14) Antonelli, D. M.; Ying, J. Y. *Angew. Chem., Int. Ed. Engl.* **1995**, *34*, 2014.

(15) Stone, V. F.; Davis, R. J. *Chem. Mater*. **1998**, *10*, 1468.

(16) On, D. T. *Langmuir* **1999**, *15*, 8561.

(17) Blanchard, J.; Schüth, F.; Trens, P.; Hudson, M. *Microporous Mesoporous Mater*. **2000**, *39*, 163.

(18) Cabrera, S.; El-Haskouri, J.; Beltrán-Portier, A.; Beltrán-Portier, D.; Marcos, M. D.; Amorós, P. *Solid State Sci.* **2000**, *2*, 513.

(19) Soler-Illia, G. J. de A. A.; Louis, A.; Sanchez, C. *Chem. Mater*. **2002**, *14*, 750.

(20) Antonelli, D. M. *Microporous Mesoporous Mater*. **1999**, *30*, 315.

(21) Wang, Y.-Q.; Chen, S.-G.; Tang, X.-H.; Palchik, O.; Zaban, A.; Koltypin, Y.; Gedanken, A. *J. Mater. Chem.* **2001**, *11*, 521.

(22) Wang, Y. Q.; Tang, X. H.; Yin, L. X.; Huang, W. P.; Hacohen, Y. R.; Gedanken, A. *Adv. Mater*. **2000**, *12*, 1183.

(23) Yoshitake, H.; Sugihara, T.; Tatsumi, T. *Chem. Mater*. **2002**, *14*, 1023.

(24) Yang, P.; Zhao, D.; Margolese, D. I.; Chmelka, B. F.; Stucky, G. D. *Nature* **1998**, *396*, 152.

(25) Yang, P.; Zhao D.; Margolese D. I.; Chmelka B. F.; Stucky, G. D. *Chem. Mater*. **1999**, *11*, 2813.

(26) Grosso, D.; Soler-Illia, G. J. de A. A.; Babonneau, F.; Sanchez, C.; Albouy, P.-A.; Brunet-Bruneau, A.; Balkenade, A. R. *Adv. Mater*. **2001**, *13*, 1085.

(27) Kluson, P.; Kacer, P.; Cajthaml, T.; Kalaji, M. *J. Mater. Chem*. **2001**, *11*, 644.

(28) Crepaldi, E. L.; Soler-Illia, G. J. de A. A.; Grosso, D.; Sanchez, C. *New J. Chem.* **2003**, *1*, 9.

(29) Yu, J.; Yu, J. C.; Ho, W.; Jiang, Z. *New J. Chem.* **2002**, *26*, 607.

(30) Fröba, M.; Muth, O.; Reller, A. *Solid State Ionics* **1997**, *101*−*103*, 249.

(31) Wainwright, M. S.; Foster, N. R. *Catal. Rev. Sci. Eng.* **1979**, *19*, 211.

(32) Lewis, K. E.; Parfitt, G. D. *Trans. Faraday Soc.* **1966**, *62*, 204.

(33) Jung, S.-H.; Kang, S.-W. *Jpn. J. Appl. Phys.* **2001**, *40*, 3147.

(34) Tanev, P. T.; Pinnavaia, T. J. *Science* **1995**, *267*, 865.

(35) Cassiers, K.; Van Der Voort, P.; Linssen, T.; Vansant, E. F.; Lebedev, O.; Van Landuyt, J. *J. Phys. Chem. B* **2003**, *107*, 3690.